

A Real-Time Monitor For TeV Transients With the LHAASO-WCDA

, G.M. Xiang^{a,b} M. Zha^{a,c,*} and J.N. Zhou^b Y. Xing^b for the LHAASO collaboration

^aKey Laboratory of Particle Astrophysics, Institute of High Energy Physics, Chinese Academy of Sciences, 100049, Beijing, China

^bKey Laboratory for Research in Galaxies and Cosmology, Shanghai Astronomical Observatory, Chinese Academy of Sciences, 200030, Shanghai, China

^cTIANFU Cosmic Ray Research of Sciences, Chengdu, Sichuan, China

E-mail: zham@ihep.ac.cn, xianggm@ihep.ac.cn

With high duty cycle and wide aperture, the Large High Altitude Air Shower Observatory - Water Cherenkov Detector Array (LHAASO-WCDA) can conduct an unbiased gamma-ray sky survey in the energy range from a few hundred GeV to 100 TeV. The sensitivity of WCDA is as high as a few percent of Crab units, which allow us to monitor the VHE variability of blazars. Once a flare exceeding the threshold is detected, an alert will be generated and follow-up analysis could be carried out. In this paper the candidate sources, the methods and current status of the monitors as well as some prospects of alert issues in the future will be presented.

38th International Cosmic Ray Conference (ICRC2023)
26 July - 3 August, 2023
Nagoya, Japan



*Speaker

1. Introduction

At present more than 60 Very High Energy(VHE) extra-galactic sources have been detected. Most of these sources belong to the blazar class of Active Galactic Nuclei (AGNs), mainly as BL Lac objects. The emission from blazar is highly variable and is characterized by a flaring behavior, in which the flux increased dramatically on various time scales, even down to the hour time scale. Many interesting studies in physics can be done on the flaring phenomenon or variability studies. For instance, spectral variations of gamma rays from the sources are used as a tool to understand the physics of the source and the acceleration model of emitted gamma rays [1, 2]. Therefore, studying or monitoring their variability with sufficiently low exposure time is necessary. And detecting and monitoring gamma ray emissions from flaring sources in the very high energy region is a very important topic in gamma-ray astronomy.

On the base of its large field of view, high duty cycle and low threshold energy, LHAASO-WCDA is a good candidate to detect and monitor the flaring phenomena. Based on reconstruction and analysis, a real-time monitoring and alerting system for selected VHE extra-galactic sources has been implemented. Data of any candidate source can be analyzed within short time after it ends the transit in the local sky. Due to the importance of studying flare, many instruments have implemented automatic program to monitoring flare, such as ARGO-YBJ [3], HAWC [4]. In this paper, we report how the flare monitor of LHAASO-WCDA works and the future plans of our monitor program.

2. The LHAASO-WCDA

The Large High Altitude Air Shower Observatory (LHAASO) is located at Haizi mountain, Daochen with altitude of 4410 m a.s.l., and $29^{\circ}21'27.6''$ N, $100^{\circ}08'19.6''$ E, Sichuan province P.R.China. The whole array is mainly composed of three sub-arrays, KiloMeter square Array(KM2A), Water Cherenkov Detector Array (WCDA) and Wide Field of View Cherenkov Telescope Array (WFCTA). LHAASO is designed for detection of air showers induced by all kinds of cosmic-ray particles with energy ranging from a few tens of GeV to a few EeV. Therefore LHAASO is a multi-purpose facility for gamma ray astronomical observation, cosmic-ray energy spectrum measurements for individual species and other wide-ranging topics associated with the cosmic-rays or air-shower phenomena. For the gamma-ray source survey, the designed sensitivity is about 0.01 CU (Crab Unit). Its wide FoV allows LHAASO to survey 1/7 of the northern sky at any moment for gamma-ray sources. With the operation in full duty cycle, LHAASO scans the entire northern hemisphere every 24 hours. The spectra of all sources in its FoV will be measured with high precision over a wide energy range from 10^{11} eV to 10^{15} eV.

WCDA consists of 3 separate pools with a total area of about 78,000 m^2 . The area of each small pools (No.1 and No.2) is $150 \times 150 m^2$ with 900 detection units ($5 \times 5 m^2$), and the area of the third pool (No.3) is $300 \times 110 m^2$ with 1320 detection units. Each detection unit is separated by black plastic curtains to block the scattered light from other

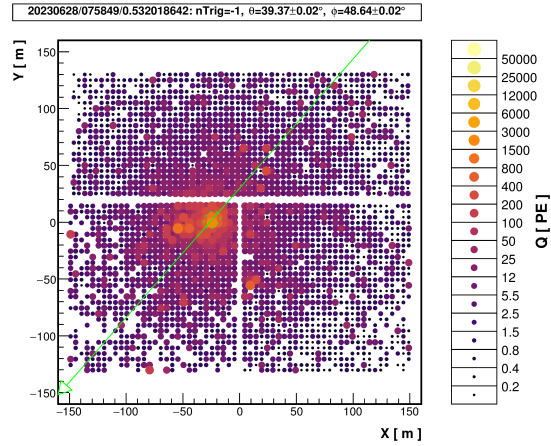


Figure 1: A example event recorded by WCDA on 28th June 2023, right panel shows the magnitude of the Npe received by each detector cell, the green line means reconstructed direction, the green circle is reconstructed shower core position.

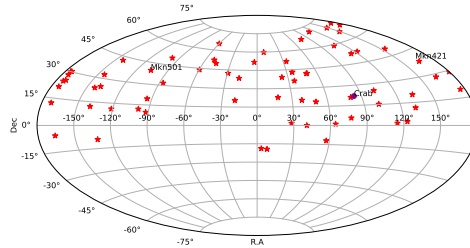


Figure 2: The sky map including all selected sources.

units. With high duty cycle and wide aperture, the WCDA's detection threshold can reach a few percent of Crab units at 300 GeV to 100 TeV energies in one year survey.

3. Monitoring scheme

3.1 Source selection

At this moment only targets with the declination between -20° and 80° are selected. The source is mainly from TeVCat [5], 68 VHE blazars listed in TeVCat is included; Besides the Crab Nebula is selected to supervise the operating status of this program. Fig.2 shows the the sky map of selected VHE sources in galactic coordinates.

3.2 Search for excess

After reconstruction, the arrival direction of events that pass the quality cuts (details in [6]) are binned in equatorial coordinates for a event map. In order to obtain the excess of gamma-ray induced showers, the "direct integration method" is used to estimate the number of background events. This method[7] uses events with the same direction in local coordinates but different arrival times to estimate the background. In this work, the

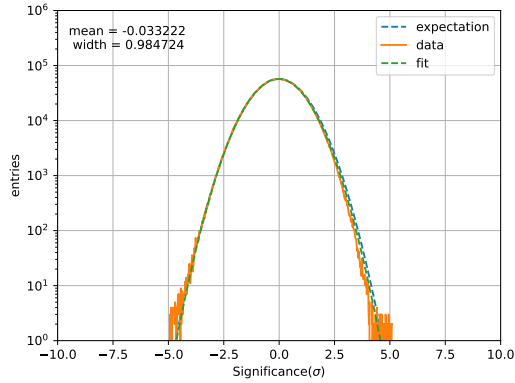


Figure 3: Significance distribution of all sky cells for 1 days data.

integrated time is 2 hours, and the events within the regions of galactic plane (latitude less than 3 deg.) and some gamma-ray sources are excluded from the background estimation.

Both event and background maps are generated using a HEALPIX [8]. For the present analysis, maps were subdivided into a grid of 1024×1024 , mean spacing between pixel centers is less than 0.06° which is small compared to the typical Point Spread Function (PSF) of this work, around 0.6° . Then the Li-Ma prescription [9] is adopted to calculate the significance. Fig.3 shows the significance distribution of all sky cells for data within one day in the year of 2023. One can find that it can be well fitted to a normal distribution, indicating that the method produced excellent background estimation.

3.3 Space and Duration search

In order to avoid source positioning problems, the maximum searching distance between the source and grid center is set as 0.1° , i.e. it is 23 searching around the selected target within 0.1° in space is employed. And there is no well-established theoretical model to understand the duration of the flaring phenomenon. In this work, each source is monitored until it leaves from the field of view of the WCDA (zenith angle less than 60 deg.). On its disappearance, the excess significance of 0.5, 1, 2, 4 transits are calculated.

3.4 Alarm threshold

The flare monitor select maximum significance in space and duration bins. Due to correlations between spatial and duration searches, there is no simple distribution to describe this distribution. A Monte Carlo simulation of search mechanism is applied to calculate the relation between false alarm rate and significance threshold. The relationship between false alarm rate for a single source, or all 66 (except Mrk 421, Mrk501) sources, and the significance threshold, named as $S_{threshold}$, is shown in Fig.4. The threshold of 4.20 and 5.00 is relative to a chance probability of once per year for a single source and all 66 sources respectively. Here the chance probability of once per year indicate that false alarms due to background fluctuations would happen once in every year. In addition, for the extra-

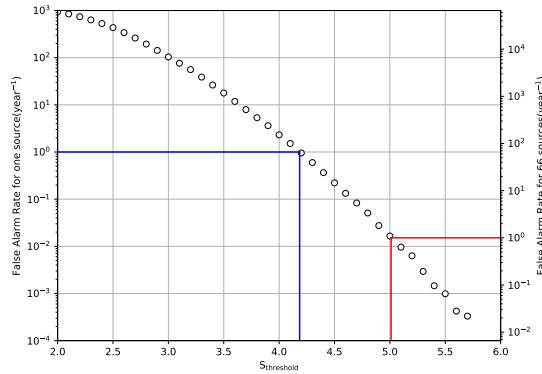


Figure 4: The false alarm rate as a function of the threshold value

galactic sources with stable strong emission, such as Mrk 421, Mrk 501, we add additional corrections to the thresholds, at least 3 factor average flux is needed to send an alert.

The above monitoring procedure has been preliminary established in the end of 2019 as just WCDA-1 data-taking. Now it is running for WCDA full array configuration. Fig.5 is the monitoring history of Mrk421 from April 2023 to June 2023. the yellow line in the figure indicates 3 factor average flux which is estimated from long-term observation. It is obvious that Mrk421 is in active status again. There are 4 flares around mjd=60055, 60075, 60090 and 60120 detected which all of them were coincident with MAXI-GSC [10]. In the other side, if there is nothing specially happen, a daily monitor summary report would be sent by Email within the working group as shown in Fig.6

4. Summary and Outlook

In this work, a real-time monitor by using LHAASO-WCDA for TeV transients of extra-galactic sources has been presented. Based on current monitor scheme, VHE flare events can be detected and monitored. Our next step works will mainly focus on two aspects. Firstly it is about new candidated sources, the Third Catalog of Hard Fermi-LAT Sources (3FHL) [11], containing 1556 objects characterized in the 10 GeV-2 TeV energy range. A majority of detected sources(79%) are associated with extra-galactic counterparts in multi-wavelength. 3FHL sources have the potential to generate VHE radiation. We are planing to pick out extragalactic sources with $z < 0.2$ as new candidated sources. Secondly it is about follow-up analysis once an alert is produced, a corresponding cross-check and multi-wavelength and global analysis could be implemented. To keep the analysis time as short as possible and to spread and to share alert and its subsequent news are important factor to be considered.

5. Acknowledgments

The authors would like to thank all staff members who work at the LHAASO site above 4400 meter above the sea level year round to maintain the detector and keep the

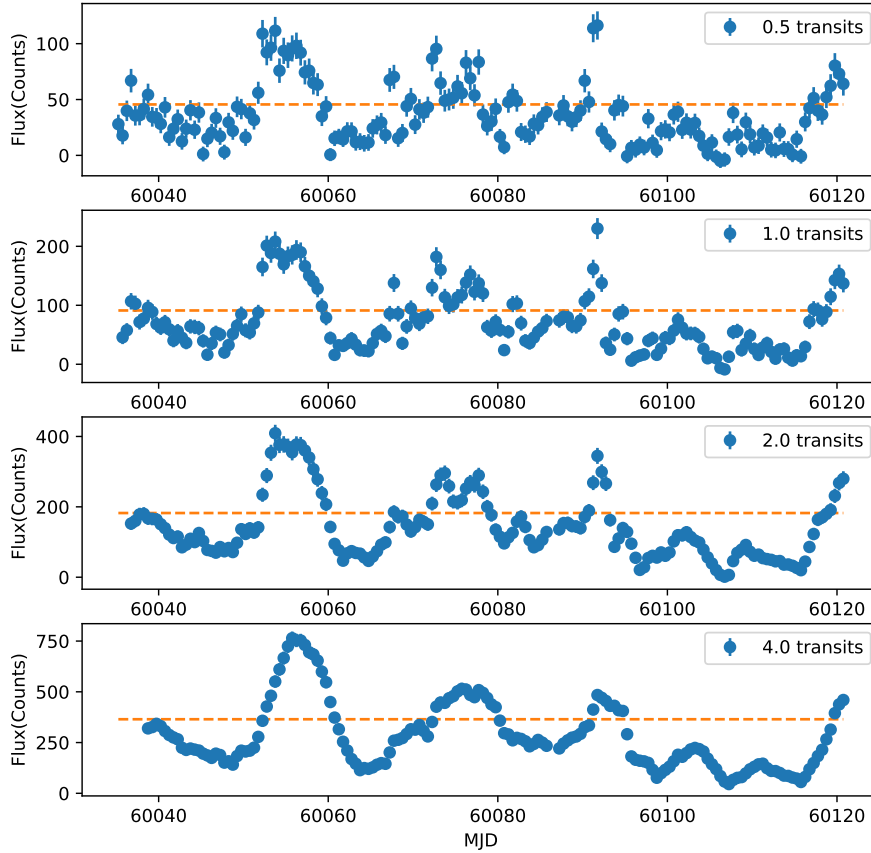


Figure 5: Monitoring history of Mrk421 from April to June in the year of 2023, the flux for 0.5, 1, 2, 4 transits are shown from top to bottom panel. The yellow line represents 3 factor average flux.

water recycling system, electricity power supply and other components of the experiment operating smoothly. We are grateful to Chengdu Management Committee of Tianfu New Area for the constant financial support for research with LHAASO data. This research work is also supported by the National Natural Science Foundation of China No.11675187, No.U1831208.

References

- [1] C. Megan Urry and Paolo Padovani. Unified Schemes for Radio-Loud Active Galactic Nuclei. , 107:803, Sep 1995;
- [2] Frank Rieger. Gamma-Ray Astrophysics in the Time Domain. *Galaxies*, 7(1):28, Jan 2019.

# name	RA	DEC	ON	BK	Fig
Markarian421	166.08	38.19	84.00	73.72	1.20
Markarian501	253.47	39.76	90.00	66.92	2.82
WComae	185.38	28.23	90.00	77.91	1.37
SHBLJ001355_9-185406	3.47	-18.89	1.00	1.20	-0.18
KUV00311-1938	8.40	-19.35	1.00	0.87	0.14
1ES0033+595	8.82	59.79	26.00	28.86	-0.53
S20109+22	18.02	22.74	64.00	71.26	-0.86
RGBJ0136+391	24.13	39.10	52.00	63.66	-1.46
RGBJ0152+017	28.14	1.78	38.00	30.18	1.42
TXS0210+515	33.57	51.75	48.00	45.86	0.32
S30218+35	35.27	35.94	72.00	71.68	0.04
3C66A	35.67	43.04	61.00	62.29	-0.16
MAGICJ0223+403	35.80	43.01	67.00	62.50	0.57
1ES0229+200	38.22	20.27	62.00	70.94	-1.06
IC310	49.18	41.32	63.00	64.32	-0.16
RBS0413	49.95	18.76	78.00	66.37	1.43
NGC1275	49.95	41.51	59.00	62.90	-0.49
1ES0347-121	57.35	-11.98	9.00	7.39	0.59
1ES0414+009	64.22	1.09	26.00	29.04	-0.56
1ES0502+675	76.98	67.62	19.00	16.00	0.75
TXS0506+056	77.35	5.70	34.00	39.86	-0.93
VERJ0521+211	80.44	21.21	67.00	70.52	-0.42
RXJ0648_7+1516	102.19	15.27	79.00	56.48	3.00
1ES0647+250	102.69	25.05	67.00	70.63	-0.43
RGBJ0710+591	107.61	59.15	21.00	29.38	-1.55
S50716+714	110.47	71.34	11.00	10.51	0.15
PKS0736+017	114.82	1.60	34.00	30.86	0.57
1ES0806+524	122.50	52.32	51.00	43.11	1.20
RBS0723	131.80	11.56	46.00	50.85	-0.68
OJ287	133.70	20.10	84.00	71.90	1.43
M82	148.97	69.68	16.00	12.56	0.97
S40954+65	149.70	65.57	19.00	18.12	0.21
1ES1011+496	153.77	49.43	54.00	50.65	0.47
Markarian180	174.11	70.16	5.00	11.37	-1.89
RXJ1136_5+6737	174.12	67.62	11.00	15.63	-1.17
3C264	176.27	19.61	68.00	66.91	0.13
TON0599	179.88	29.25	84.00	75.74	0.95
1ES1218+304	185.36	30.19	80.00	74.14	0.68
1ES1215+303	184.45	30.10	64.00	73.39	-1.10
MS1221_8+2452	186.10	24.61	81.00	73.77	0.84
4C+21_35	186.22	21.38	59.00	70.45	-1.36
S31227+25	187.56	25.30	68.00	73.88	-0.68
M87	187.70	12.40	64.00	53.16	1.49
3C279	194.05	-5.79	17.00	14.02	0.80
B21420+32	215.62	32.39	65.00	74.42	-1.09
PKS1424+240	216.75	23.79	57.00	71.13	-1.68
H1426+428	217.13	42.67	53.00	58.84	-0.76
1ES1440+122	220.81	12.00	58.00	52.18	0.81
PKS1441+25	220.98	25.03	85.00	73.03	1.40
PKS1510-089	228.22	-9.11	10.00	9.95	0.02
PG1553+113	238.93	11.19	47.00	49.72	-0.39
H1722+119	261.27	11.87	36.00	50.17	-2.00
1ES1727+502	262.07	50.22	64.00	48.63	2.20
1ES1741+196	266.00	19.55	72.00	62.92	1.15
0T081	267.88	9.65	51.00	45.64	0.79
B21811+31	273.40	31.74	76.00	74.74	0.15
.....					

Figure 6: One Daily summary report from monitor scheme.

- [3] ARGO-YBJ Collaboration, NIMA, 659(1):428–433, 2011.
- [4] HAWC Collaboration, arXiv e-print, arXiv:1508.05399, 2015.
- [5] Tevcat. <http://tevcat.uchicago.edu/>.
- [6] LHAASO Collaboration, arXiv e-print, arXiv:2305.17030, 2023.
- [7] Atkins, R. W., et al., ApJ 595 (2003) 803.
- [8] Gorski, K.M. et al., ApJ 622 (2005) 759.
- [9] T.P. Li, Y.Q. Ma, APJ 272 (1983)317.
- [10] <http://maxi.riken.jp/top/index.html>
- [11] Fermi-LAT Collaboration, arXiv e-print, arXiv:1702.00664, 2017.